Mem. Natl Inst. Polar Res., Spec. Issue, **51**, 387–394, 1996

Scientific Paper

INTERNAL LAYERING DETECTED BY MICROWAVE ICE-RADAR IN THE ARCTIC ICE CAP

Seiho URATSUKA[1], Hideo MAENO[1], Takeshi SUITZ[1], David A. FISHER[2], Kumiko GOTO-AZUMA[3] and Shinji MAE[4]

[1]*Communications Research Laboratory, 2–1, Nukui-kitamachi 4-chome, Koganei-shi, Tokyo 184*
[2]*Geological Survey of Canada, 601 Booth St., Ottawa, Ontario K1A 0E8, Canada*
[3]*Nagaoka Institute of Snow and Ice Studies, 187–16, Maeyama, Suyoshi-cho, Nagaoka 940*
[4]*Faculty of Engineering, Hokkaido University, Kita-13, Nishi-8, Kita-ku, Sapporo 060*

Abstract: Radar observations were carried out on the Agassiz ice cap in Canadian arctic territory using a newly developed high resolution ice-radar. The radar employed a microwave frequency (L-band) in order to realize resolution of less than 1 m. Actual range resolution of the radar is about 63 cm in ice. The radar can observe the bedrock topography and internal echoes with high resolution. Signals from bedrock up to 500 meters in depth were detected. The attenuation coefficient in the L-band frequency was calculated to be 0.05 dB/m. Internal ice layers were observed from about 50 m to 200 m in depth. Internal layers detected by the radar were compared to the electrical conductivity of an ice core measured by ECM at the summit of the ice cap with almost the same resolution. Each peak of the radar echo corresponded to an ECM peak, but the relationship between echo intensity and ECM intensity is not clear.

1. Introduction

Historical climate events are being recorded in the polar ice sheet and ice cap. Ice core analysis is one of the best ways to reveal ancient climate. However, drilling an ice core requires a great deal of effort and consequently ice samples are very limited. Also, it is not easy to analyze the correspondence of event layers among ice cores.

On the other hand, many VHF radar observations made in order to measure ice thickness have detected echoes from internal ice interfaces (GUDMANDSEN, 1975). Most of them have a stratified pattern. It is obvious that the internal echoes are caused by dielectric change due to ice properties. One possibility of the cause is acidity. Acidity events in ice cores can be detected by measuring the conductivity of ice samples. Most of the more highly conductive layers were assumed to correspond to volcanic ash at one time. On the contrary, FUJITA and MAE (1994) suggested that the ice structure pattern may cause the internal echoes. URATSUKA *et al.* (1996) found that layered echoes disappear near the grounding line. This fact makes it difficult to explain the echoes as being caused by acidity.

Some studies (GUDMANDSEN, 1975; MILLAR, 1981) have tried to compare ice core data with ice radar echoes, but the difference in resolution between ice cores (less than 1 cm) and ice radar (more than 10 m) prevented one-to-one correspondence: one range gate of radar includes many volcanic events.

The main purpose of this study is to reveal, by radar, (1) the three dimensional structure of ice event layers found in ice cores drilled at the site. This is useful for comparing ice cores which are sampled at different places, and also for inferring ice dynamics by tracing a layer, because a layer indicates the same age. And also, to discuss on (2) the mechanism of scattering from the internal layers, from a detailed comparison between radar echo and ice core data on the dielectric properties.

The first ground-based observation had been planned at the Agassiz ice cap, because many ice core samples drilled by the Geological Survey of Canada are available and ice thickness is not larger than 500 m.

2. High Resolution Ice-radar

Because the objective is focused on the internal layers of a shallow ice sheet or ice cap, the radar system is required to have several characteristics: (1) high resolution, (2) compactness, and (3) small power supply, but (4) deep penetration ability is not needed. In order to realize the above requirements, we adopt some key characteristics:(1) center frequency of 1.257 GHz (L-band), (2) FM chirped pulse compression, and (3) fast digitizing.

Ice-radar using microwaves was proposed before this experiment by COOPER *et al.* (1976), but they observed only lake ice. Utilizing microwaves are advantage in forming very short pulses to obtain high resolution, but attenuation in ice increases at higher frequency. Therefore, it is difficult to obtain a good signal to noise ratio (SNR) with small transmitted power. A pulse compression technique was introduced for ice-radar of 150 MHz by RAJU *et al.* (1990). This technique reduces the resolution and equivalent SNR.

The principal characteristics of this radar are listed in Table 1. Using a compression technique, the effective pulse width is 7.5 ns, with 63 cm range resolution in ice. Radar video signals were digitized and averaged by a high speed digitizing oscilloscope and recorded on floppy disks.

Table 1. Major specifications and performances of L-band high resolution ice radar.

Transmitter	Frequency	1.2575 GHz	
	Peak power	10 W	667 W (effective)
	Pulse	FM Chirp	
		500 ns (extn.)	7.5 ns(compr.)
	PRF	1 kHz	
Receiver	Smin	–88 dBm	
	Band width	270 MHz	
	NF	2.5 dB	
Antenna	1.2 m Parabora		
	Beam	17 degree	
	Gain	19 dBi	

3. Observation at the Agassiz Ice Cap

The Agassiz ice cap is located around 80.7°N, 73.1°E on Ellesmere Island and has a gently undulating surface. Figure 1 shows a topographic map of the areas around Agassiz ice cap. The observations using the ice radar system were carried out in April and May 1994 at the ice cap. Thick lines in Fig. 1 indicate the observation trajectory. Big spots beside the thick lines indicate the core sites. The site called A is the summit of this ice cap and site C is 2 km south of the summit. Radar observations were carried out along these trajectories 25 m apart. The radar antenna was mounted on a wooden sledge and faced downward, and the transmitter and receiver units and data archiving unit were put into a heating box on the sledge. These sledges are driven by a skidoo as shown in Fig. 2.

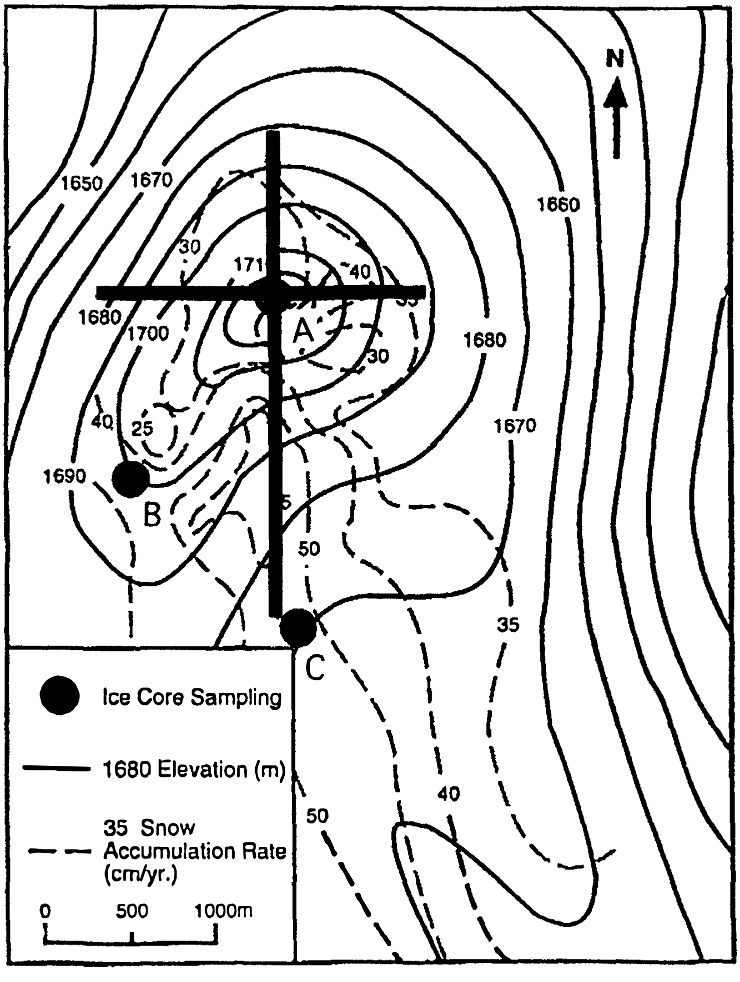

Fig. 1. Surface topography map around the summit of the Agassiz ice cap. Solid curves show topographic contours and dashed curves show annual accumulation rate. Thick lines indicate the radar observation route; big spots are locations of ice core sampling points.

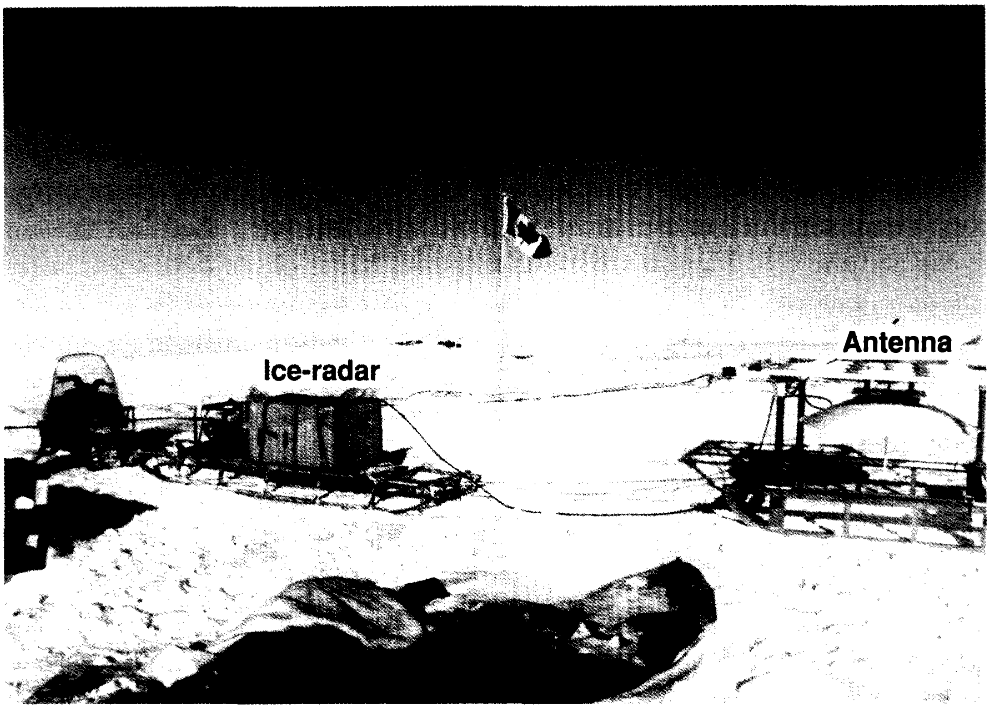

Fig. 2. Observations in progress at the summit of the Agassiz ice cap. Instruments are kept within the heating box on the first sledge after the skidoo, and a 1.2 m diameter parabola antenna for the L-band is mounted on the next sledge.

4. Cross Sectional Over-view

Figure 3 shows preliminary results of the radar echo in Z-scope form along the north-south line and west-east line in Fig. 1. In this figure, pre-processing for removing noise and reduce dynamic range in the ice region is not complete. However, we can find the internal and basal echoes in it. First, we can see dome-shaped bedrock topography very clearly. The summit of the bedrock is directly below the surface summit.

The maximum range of radar echo from the bedrock is about 400 m at the Agassiz ice cap, and 500 m at the other ice cap, which indicates that the L-band frequency is useful for utilizing the ice-radar system for shallow ice caps. The peak power of the transmitted pulse was only 10 W. If we amplify the peak power to 1 kW, the penetration will be better. Using 0.05 dB/m of attenuation coefficient at this frequency, the maximum penetration is estimated to be 700 m.

The attenuation coefficient can be calculated by measuring the depth dependence of echo strength from the bedrock using the radar equation proposed by URATSUKA *et al.* (1989). In this observation, the attenuation coefficient is 0.05 dB/m, corresponding to 80 m in penetration depth and 3×10^{-4} in the imaginary part of the refractive index. This result corresponds to the –5°C case in the laboratory measurements by Westphal's diagram (WARREN, 1981).

Internal echoes are found in layered form about 1 km south of the summit in the Fig. 3. However, the layered structure is not clear around the summit. The reason for unclear layering is considered as follows: The foot-print of the antenna beam is smaller

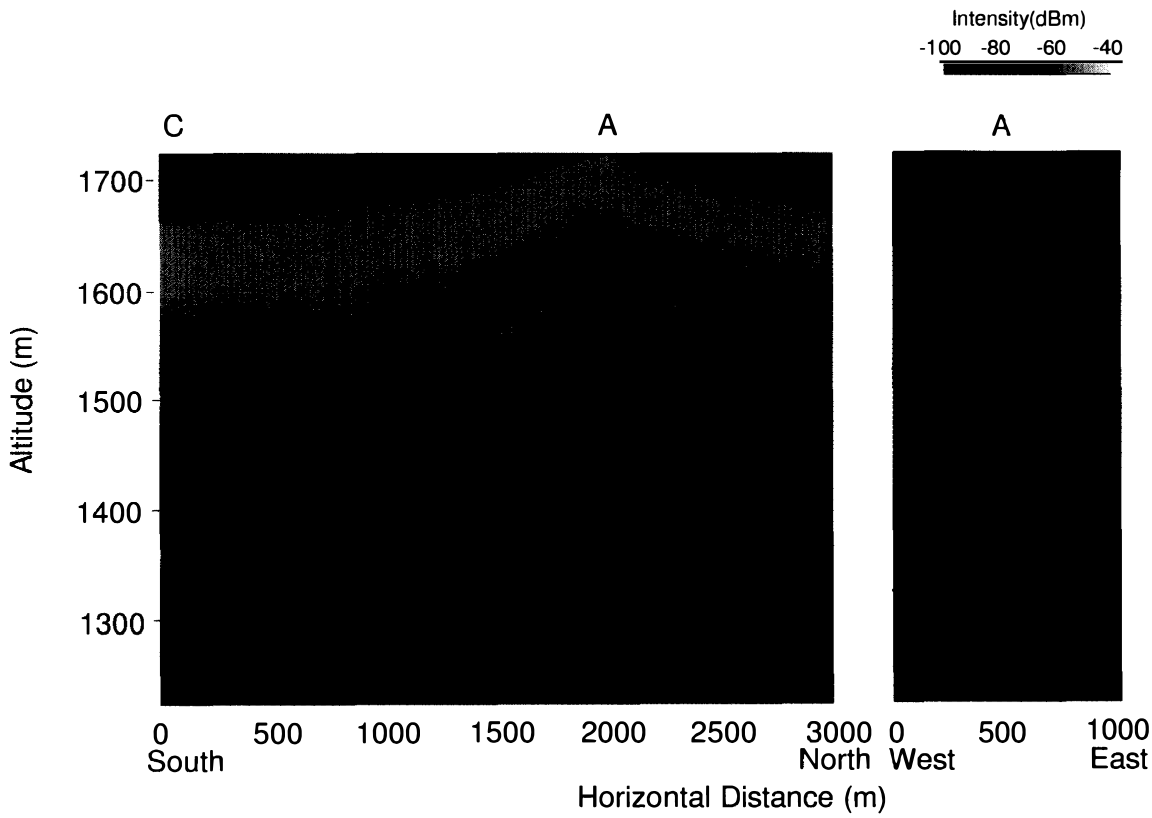

Fig. 3. Preliminary results of ice radar measurement in Z-scope form. The vertical scale is converted from delay time to altitude from sea level.

than 15 m at depths shallower than 200 m. On the other hand, the separation of observation points is 25 m. This means that the coverages of observation in the horizontal plane do not over-lapped. So the correlation between the nearest points might be bad.

5. Internal Layering by Radar

Internal echoes were detected in enough strength until about 200 m. Figure 4 shows an example at site C on Fig. 1. The largest peak at 300 m depth is an echo from the bedrock. We can see very fine peaks from 80 m to 200 m depth in this figure. Echoes from the surface to about 80 m depth are saturated, because the surface echoes were strongly affected with expanded pulse. The peaks between 80 m and the bedrock position (200 m) had good resolution (less than 1 m).

Before a detailed comparison between ice core data and radar data, depth scaling correction of radar data was carried out using a density profile obtained from an ice core at the summit. The dielectric constant at the firn is mainly controlled by the density. We obtained the following correction curves using a dielectric constant model for density proposed by Looyenga (Retzlaff and Bentley, 1993) with the density profiles at sites A and C. Figure 5 shows correction curves from the data of sites A and C with the case of constant refractive index. These curves are nearly linear and very close in the range of 0.4 to 2.2 ns delay time. Then we use a convenient equation between depth d and delay

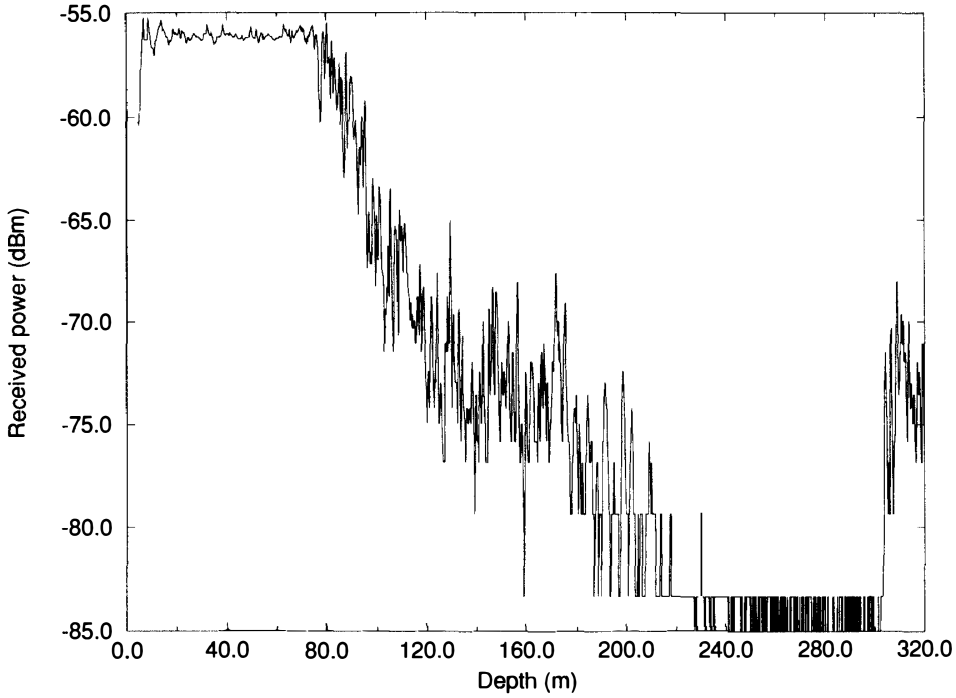

Fig. 4. An example of a radar signal in A-scope form. The location of the data is 1 km south of the summit. The peak around 300 m is from the bottom. The signals in the depth range from 0 to 80 m are saturated. The fine peaks in the range between 80 and 200 m are received from the internal ice.

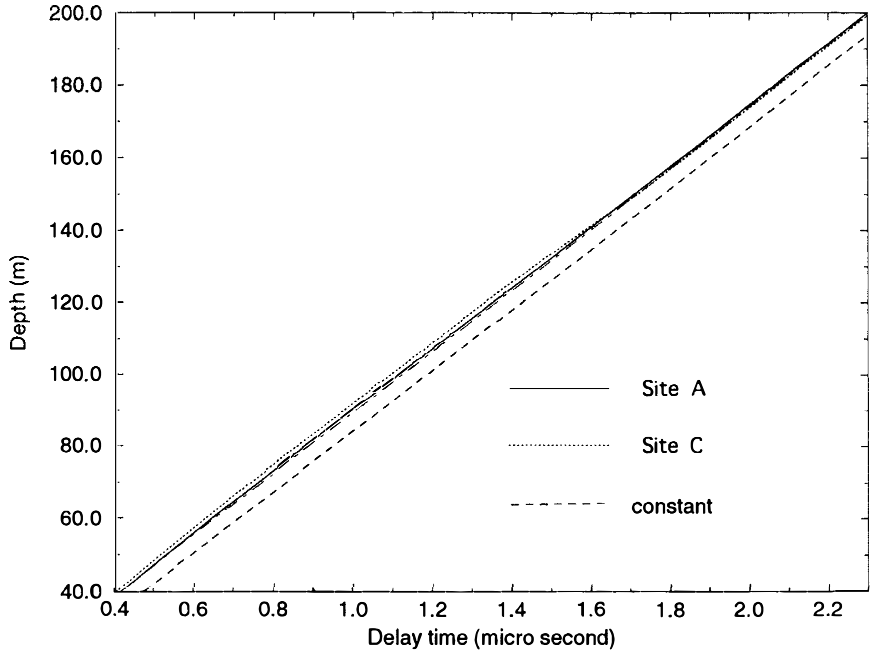

Fig. 5. Depth scaling curves by the Looyenga model using the data from site A (strait) and site C (dotted), and a constant model (dashed).

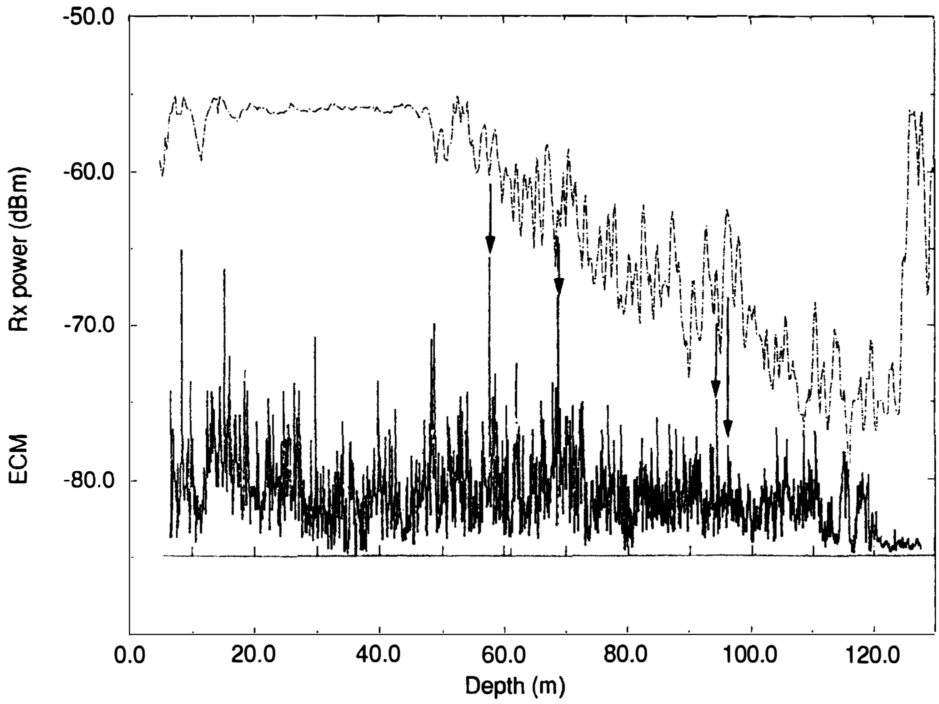

Fig. 6. Comparison between radar echoes observed at site A (upper curve) and the ECM data from the ice core at the same position (lower curve). Some strong peak of ECM data correspond to radar echoes (shown by arrows), but the relation to the intensity is not clear.

time t.

$$d = 4.76 + 8.47 \times t.$$

Figure 4 already employed the above equation. Figure 6 shows the radar echo at site A with data from the electric conductivity measurement (ECM) on the same depth scale. At site A, the ice thickness was 126 m. Radar data are calibrated to the received power in dBm, but no correction is made for ice attenuation. The ECM data are not calibrated, intensities are relative values of conductivity, and small peaks include noise, but strong peaks indicate high conductivity qualitatively. Some of the strong peaks are identified to correlate with historical volcanic activity (FISHER and KOERNER, 1994).

Multiple peaks are found between 40 m and 126 m in the radar data; some of them appear to correspond to the peaks of the ECM data. However, there is not a clear dependence between radar intensity and conductivity, as would be expected if the radar signal decreases with depth by ice attenuation. This suggests that the cause of the internal echoes is not only acidity.

6. Concluding Remarks

This first observation which employed an ice-radar system confirmed the availability of the L-band frequency for studying internal layering and shallow bedrock with high resolution. However, the layered image in Z scope image was not clear as we expected. We should observe with gaps between measurements shorter than the beam foot-print. A comparison between ice-radar and ECM data was given with compatible resolution. Strong conductivity is expected to reflect a strong echo, but the data show that conductivity is not the only cause of internal echoes. Further investigation using other ice core data should be conducted.

References

COOPER, D.W., MUELLER, R.A. and SCERTLER, R.J. (1976): Remote profiling of lake ice using an S-band short-pulse radar aboard an all-terrain vehicle. Radio Sci., **11**, 375–381.

FISHER, D.A. and KOERNER, R.M. (1994): Signal and noise in four ice-core records from Agassiz Ice Cap, Ellesmere Island, Canada: Details of the last millennium for stable isotopes, melt and solid conductivity. Holocene, **4**, 113–120.

FUJITA, S. and MAE, S. (1994): Causes and nature of ice-sheet radio-echo internal reflections estimated from the dielectric properties of ice. Ann. Glaciol., **20**, 80–86.

GUDMANDSEN, P. (1975): Layer echoes in polar ice sheet. J. Glaciol., **15**, 95–100.

MILLAR, D.H.M. (1981): Radio-echo layering in polar ice sheets and past volcanic activity. Nature, **292**, 441–445.

RETZLAFF, R. and BENTLEY, C.R. (1993): Timing of stagnation of Ice Stream C, West Antarctica, from short-pulse radar studies of buried surface crevasses. J. Glaciol., **39**, 553–561.

RAJU, G., XIN, W. and MOORE, R.K. (1990): Instruments and method: Design, development, field observations, and preliminary results of the coherent Antarctic radar depth sounder (CARD) of the University of Kansas, USA. J. Glaciol., **36**, 247–254.

URATSUKA, S., NISHIO, F., OHMAE, H. and MAE, S. (1989): Radio scattering characteristics of Antarctic ice sheet using airborne radio echo sounding data. Proc. NIPR Symp. Polar Meteorol. Glaciol., **2**, 142–151.

URATSUKA, S., NISHIO, F. and MAE, S. (1996): Internal and basal ice changes near the grounding line derived from radio echo sounding. J. Glaciol., **42**, 103–109.

WARREN, S.G. (1981): Optical constants of ice from the ultraviolet to the microwave. Appl. Opt., **23**, 1206–1225.

(Received January 8, 1996; Revised manuscript accepted May 17, 1996)